On the Impact of Granularity of Space-based Urban CO$_2$ Emissions in Urban Atmospheric Inversions: A Case Study for Indianapolis, IN

Tomohiro Oda[1,2*], Thomas Lauvaux[3], Dengsheng Lu[4], Preeti Rao[5], Natasha L. Miles[3], Scott J. Richardson[3] and Kevin R. Gurney[6]

1. Global Modeling and Assimilation Office, NASA Goddard Space Flight Center, Greenbelt, Maryland, USA
2. Goddard Earth Sciences Technologies and Research, Universities Space Research Association, Columbia, Maryland, USA
3. Department of Meteorology and Atmospheric Science, The Pennsylvania State University, University Park, Pennsylvania, USA
4. Michigan State University, East Lansing, Michigan, USA
5. NASA Jet Propulsion Laboratory, Pasadena, California, USA
6. School of Life Sciences, Arizona State University, Tempe, Arizona, USA

Corresponding author: T. Oda (tomohiro.oda@nasa.gov)

Abstract

Quantifying greenhouse gas (GHG) emissions from cities is a key challenge towards effective emissions management. An inversion analysis from the INdianapolis FLUX experiment (INFLUX) project, as the first of its kind, has achieved a top-down emission estimate for a single city using CO$_2$ data collected by the dense tower network deployed across the city. However, city-level emission data, used as *a priori* emissions, are also a key component in the atmospheric inversion framework. Currently, fine-grained emission inventories (EIs) able to resolve GHG city emissions at high spatial resolution, are only available for few major cities across the globe. Following the INFLUX inversion case with a global 1×1 km ODIAC fossil fuel CO$_2$ emission dataset, we further improved the ODIAC emission field and examined its utility as a prior for the city scale inversion. We disaggregated the 1×1 km ODIAC non-point source emissions using geospatial datasets such as the global road network data and satellite-data driven surface imperviousness data to a 30×30 m resolution. We assessed the impact of the improved emission

1

field on the inversion result, relative to priors in previous studies (Hestia and ODIAC). The posterior total emission estimate (5.1 MtC/yr) remains statistically similar to the previous estimate with ODIAC (5.3 MtC/yr). However, the distribution of the flux corrections was very close to those of Hestia inversion and the model-observation mismatches were significantly reduced both in forward and inverse runs, even without hourly temporal changes in emissions. EIs reported by cities often do not have estimates of spatial extents. Thus, emission disaggregation is a required step when verifying those reported emissions using atmospheric models. Our approach offers gridded emission estimates for global cities that could serves as a prior for inversion, even without locally reported EIs in a systematic way to support city-level Measuring, Reporting and Verification (MRV) practice implementation.

1. Introduction

Cities account for more than 70% of global total greenhouse gas (GHG) emissions. Quantifying GHG emissions from cities, which are often the smallest administrative unit, is thus a key challenge towards effective emissions management. Emission inventories (EI) are a fundamental tool to keep track of emission changes (e.g., national emission inventory (NEI)). However, most cities do not even compile EIs although they have been recognized as practical emission reduction target, even when motivated by international consortiums (e.g., C40 cities climate leadership group). Moreover, EIs are prone to systematic biases from both the emission calculation methodology and the inadequate quality of the underlying activity data (e.g., Guan *et al.* 2012; Liu *et al.* 2015). In the absence of a transparent protocol to provide reliable activity data and a robust calibration method, EIs remain uncertain, therefore limited in their ability to measure GHG emission reduction efforts in metropolitan areas (Hutyra *et al.*, 2014). At the country scale (e.g., Kyoto Protocol), EIs aim to determine the level of contribution of various sectors to national carbon budgets thereby supporting the implementation of carbon mitigation for which accurate quantification of emissions is of major importance. The authors believe it is important for the science community to contribute to establishing a framework prefacing the implementation of a complete Monitoring/Reporting/Verification (MRV) practice for cities, guiding stakeholders and emission management policies.

Cities' roles for emission management and emission reduction potential have been identified. However, only few megacities are compiling their EI with the required granularity. Especially, quantification of emissions from cities is preferably done by developing fine-grained bottom-up EI where emission accounting and geolocating are available at the same spatial scale, as done by Gurney *et al.* (2012) as opposed to most gridded datasets based on disaggregation of national/sectoral emissions (e.g., Andres *et al.*, 1996; Olivier *et al.*, 2005; Janssens-Maenhout *et*

al., 2012; Rayner *et al*., 2010; Oda and Maksyutov 2011; Kurokawa *et al*., 2013; Asefi-Najafabady *et al*., 2014). The links between human activities and emissions described in a bottom-up framework provide more information on energy use than top-down estimates, which are limited by the ambiguity of mixed source signals in atmospheric observations. However, the development of fine scale EI is often labor intensive and difficult to be completed in a timely manner (i.e., annual basis). In fact, such fine-grained city emission datasets are only available for few locations. Over the continental US, only few EI's have been compiled at the building-level resolution: Indianapolis (Gurney *et al.*, 2012), Los Angeles (Feng *et al*., 2016), Baltimore (Gurney *et al.*, in preparation) and Salt Lake City (Patarasuk *et al.*, 2016). Furthermore, error quantification and characterization associated with EI's is another emerging issue (e.g., Andres *et al*., 2016). Especially for fine-grained EI's, uncertainty assessment is non-trivial and involves complex parametric and structural uncertainties (Gurney et al., same issue). Those information should be included in city scale inversion to obtain robust city emission estimates (Lauvaux *et al.* 2016).

Beyond their original use for city emission accounting, EI is also a key component in top-down methods as they provide a first guess in the optimization problem to help identify the source distribution (Enting, 1995). The use of atmospheric data to verify EI's has been encouraged by several studies (e.g., Nisbet and Weiss, 2010; Pacala *et al.*, 2010) and supported by the analysis of various types of instrumentation (e.g., Kort *et al.,* 2010, Janardanan *et al.,* 2016 for satellite CO_2 data; Basu *et al.,* 2016 for C^{14} radiocarbon data). Recently, an inversion analysis from the Indianapolis Flux experiment (INFLUX) project, as the first of its kind, has achieved a top-down emission estimate for a single city and demonstrated the use of atmospheric CO_2 tower data to constrain urban emissions (Lauvaux *et al.*, 2016). The inversion system used the "Hestia" fine-grained emission dataset (Gurney *et al.*, 2012, data available from http://hestia.project.asu.edu/) as *a priori* emission and derived emission corrections using atmospheric CO_2 data from the dense tower network within the city domain. The inverse methodology produced 1-km resolution adjustments to the first guess (Hestia) modifying the total emissions by about 20%, a statistically significant change reflecting possible discrepancies between the two methods including the presence of additional sources beyond anthropogenic emitters (e.g., soil respiration - Gurney *et al.*, same issue). The study also illustrated the impact of assimilating coarser resolution prior emissions taken from the Open-source Data Inventory for Anthropogenic CO_2 (ODIAC) global 1×1 km fossil fuel emissions dataset (Oda and Maksyutov, 2011; Oda *et al.*, 2016, data available from http://db.cger.nies.go.jp/dataset/ODIAC/) and its impact on the spatial structures of the emission corrections.

Potentially being applicable to any cities, top down approaches are currently being tested across few metropolitan areas (e.g., Feng *et al.*, 2016), mostly due to the lack of atmospheric GHG networks to constrain city emissions. The deployment of ground-based instruments require an existing infrastructure (i.e. accessible tall towers or high buildings) and expert knowledge to calibrate the instruments (Richardson *et al.*, same issue). Other observing strategies such as future satellite missions (e.g., Orbiting Carbon Observatory-3 - Eldering, 2015; CarbonSAT - Buchwitz *et al.*, 2013; GeoCARB - Polonsky *et al.*, 2014) are currently under development and could provide the required constraint on urban emissions in the near future. In this study, we present the space-based emission field at fine resolution to inform a top-down urban-scale framework. We evaluate the product against an existing fine-grained EI, Hestia, and assess the impact of the fine-scale structures on the posterior emissions estimate. The original ODIAC emissions is a global data set based on disaggregation of national emissions using point source profiles (power plant emission estimates and geolocation) and satellite-observed nighttime lights (e.g., Oda and Maksyutov, 2011). The total emission for the Indianapolis domain taken from ODIAC for *a priori* was remarkably close to Hestia as shown by Lauvaux *et al.* (2016), meaning the national emission disaggregation in ODIAC was sufficient for an annual estimate of the whole-city emissions. We present here an improved product at a higher level of granularity with the ambition of achieving the required accuracy in emissions estimates, i.e. sufficient to inform city-scale mitigation policies (i.e. less than 10% annually). However, the emission disaggregation technique using proxy geospatial data, while applicable to the large scale, is limited by the spatial heterogeneity of sources at finer scales. Therefore, proxy data-based emission disaggregation approaches would not work at higher resolutions, especially at the city level when light intensity and population are decorrelated from large emitters. We thus focus on creating better emission spatial structures by determining locations of specific aggregated emission sectors and attempt to make the method applicable to other metropolitan areas.

2. Methods

2.1 Urban emission field

We created a fine-grained emission field from the ODIAC emissions used in Lauvaux *et al.* (2016). Following the emission disaggregation commonly done in global and region gridded EI studies (e.g. Streets *et al.* 2000; Janssens-Maenhout *et al.* 2012; Kueren *et al.* 2014), city emission fields can be approximated by three principal emission type components: point, line and diffused (area) emission sources. Table 1 shows the sector emission breakdown for Hestia. Values are updated from Gurney *et al.* (2012). It is often fairly straightforward to categorize emissions into few major sectors. For Indianapolis, and likely for many other cities over North

America, emissions from transportation can account for a major fraction of the city total (about half - or 49 % - for Indianapolis). In the original ODIAC emissions, power plant emissions, which are often the major emitting sector at the national scale, are already distributed using geolocation of power plants taken from CARMA (www.carma.org) (Oda and Maksyutov, 2011; Oda *et al.* 2016). The transportation sector emissions are distributed as a diffused source. Thus, we preserved the power plant emission information from the ODIAC dataset and disaggregated the non-point source emissions (total minus point source emissions) using geospatial datasets. We used both the global road network data and satellite-data driven surface imperviousness data at 30×30 m resolution to generate a final product at a spatial scale similar to Hestia. We distributed the residual (non-point emissions) using the Global Roads Open Access Data Set (gROADS) v1 developed by the SocioEconomic Data and Applications Center (SEDAC) (CIESIN/ITOS/University of Georgia, 2013, http://sedac.ciesin.columbia.edu/data/set/groads-global-roads-open-access-v1) for transportation sector emissions (i.e. line source emissions) and used the satellite-data driven 30m surface imperviousness data (National Land Cover Dataset (NLCD) 2011 http://www.mrlc.gov/nlcd2011.php) for diffused source emissions (i.e. area source emissions). ODIAC does not distinguish emissions from the different sectors as emission estimates are based on country scale fuel consumption statistics (Oda *et al.,* 2016). In this study, we calculated the fraction of transportation emissions using Hestia (see Table 1). The sectoral emission approach is applicable to any city assuming that sectoral total estimates are available. If not, an average of sectoral contributions from other cities across the country should provide a fairly similar distribution. The impervious surface used here indicate four levels of development (high, medium, low and open space, see Figure 1), but the four categories are aggregated to one as the surface imperviousness does not directly inform CO_2 emission sectors (e.g. industrial, residential and commercial), but potential locations for area sources. We thus used population data taken from Census (www.census.gov for the year 2011) to create spatial gradient on sector emission areas indicated by gROAD data and impervious data. The use of population is a classic proxy for human emissions (e.g., Andres *et al.*, 1996) even applied for transportation emission (e.g., Olivier *et al.*, 2002) as population and traffic density are highly correlated. The use of population data is therefore a reasonable approach as a first order approximation. We found a difference of 0.3% in total emissions when projecting our 1×1 km ODIAC into the impervious surface data fields (30m resolution). We corrected the iODIAC emissions of the difference by adjusting the entire field.

Table 1. A summary of annual total sectoral emissions indicated by Hestia. Values are updated from Gurney *et al*. (2012).

Hestial emission sector	Type	Emissions (tC/yr)	Share (%)
OnRoad	Line	3,360,000	49.2%
Electricity Production	Point	1,362,000	19.9%
Industrial NonPoint	Area	492,000	7.2%
NonRoad	Area	477,000	7.0%
Residential NonPoint	Area	458,000	6.7%
Commercial NonPoint	point	369,000	5.4%
Industrial Point	Point	188,000	2.8%
Airport	Point	82,000	1.2%
Commercial Point	point	25,000	0.4%
Railroad	Line	21,000	0.3%
Total	-	6,835,000	100.0%

2.2 INFLUX urban inversion system

The flux inversion analyses in this study were done using the urban high-resolution atmospheric CO_2 inversion system developed by Lauvaux *et al.* (2016). The urban inversion system is built around the Weather Research Forecasting model coupled with Chemistry (WRF-Chem) modified for passive tracers described as Lauvaux *et al.* (2012). The version of WRF model used in Lauvaux et al. (2016) has Four Dimensional Data Assimilation (FDDA) capability and the World Meteorological Organization (WMO) observations were assimilated in order to simulate atmospheric CO_2 concentration with the best accurate meteorological conditions (Deng *et al.*, same issue). Lauvaux *et al.* (2016) used three WRF model grid configurations in nested mode (9km, 3km and 1km, see Figure 1 of Lauvaux *et al.*, 2016). This study focuses on the Indianapolis metropolitan area that is defined by 87 × 87 grid points at 1km resolution. The urban inversion system employs the Lagrangian Particle Dispersion Model (LPDM) described by Uliasz (1994) as an adjoint model for the WRF-Chem model. Lagrangian particles are released from CO_2 observation locations and transported backward in time to yield the contributions from surface fluxes and boundary contributions. As in Lauvaux *et al.* (2016), we used CO_2 data from nine towers of the INFLUX network, all of them operational over the period September 2012 to April 2013 (Miles *et al.*, same issue). The system assimilates CO_2 data and solves for 5-day corrections to surface anthropogenic emissions over the dormant season during which the

biospheric contribution is small (about 5% of the total CO_2 emissions, reported by Turnbull *et al.,* 2015). Additional modeling details are available in Lauvaux *et al.* (2016).

We will evaluate the different prior emissions by computing the final mismatch in CO_2 mixing ratios referred here as goodness-of-fit after inversion, both over the whole city and for each individual tower site. Because prior error covariances are also constructed according to the prior emissions, the goodness-of-fit depends on the distribution of sources across the inversion domain and their associated errors. The error variances will be a function of the emissions for each pixel whereas the error covariances will correspond to an exponentially decaying function assuming a correlation length scale of 4 km between urban pixels (similar to Lauvaux *et al.,* 2016). We note here that inverse emissions depend on the a priori but the relative performances will reflect the consistency between atmospheric data and the different prior emission products. Therefore, higher correlations between the posterior mixing ratios and the observations are evidences of a better agreement between the prior emissions and the true fluxes.

3. Results and discussions

3.1 Impervious data as a proxy for diffused sources

Figure 1 shows the impervious surface data over Indianapolis. We extracted three categories that indicate the level of development (high, medium and low) and a category for open space. According to NCDC categorization (http://www.mrlc.gov/nlcd06_leg.php), high density indicates 80-100% imperviousness, medium indicates 50-79%, low indicates 20-49% and open space indicates less than 20%. Although a single category is unlikely to correspond to one particular emissions sector, the city structures are clearly depicted with developed areas and open spaces, the major road transport network (e.g., beltway and interstate highways) and blocky patterns in residential areas. Compared to the spatial structures of ODIAC (see Figure 2a), the use of impervious data significantly reduces the mapping error by distributing the emissions over well-identified urban areas rather than smoothed zones overlapping with non-emitting areas. The impervious data might be able to identify particular emission sectors, but no clear relationship between the imperviousness categories and emission sectors can be established. In this study, we aggregated the four imperviousness categories and used them with population density maps as a proxy for diffused emissions.
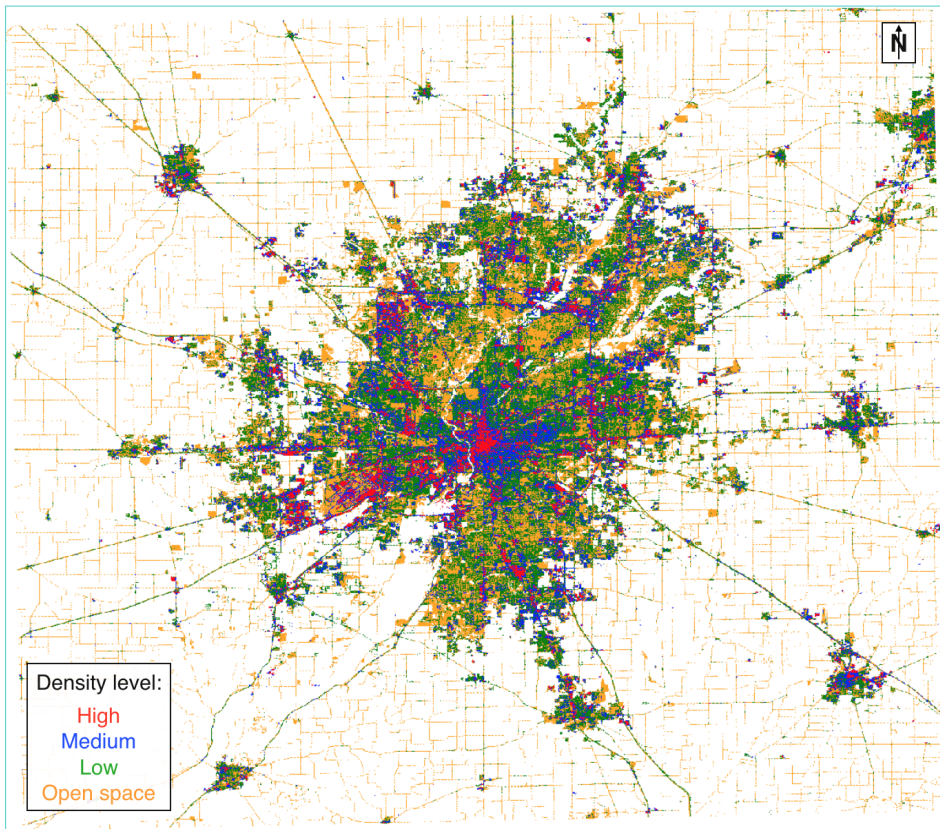
Figure 1. Impervious data over Indianapolis, IN. Data was taken from the National Land Cover Dataset (NLCD, http://www.mrlc.gov/nlcd2011.php). The impervious data indicates four different levels of developed surface: high intensity (red), medium intensity (blue), low intensity (green) and open-space. According to the NCDC categorization (http://www.mrlc.gov/nlcd06_leg.php), high density indicates 80-100% imperviousness, medium indicates 50-79%, low indicates 20-49% and open space indicates less than 20%.

3.2 30×30m improved ODIAC emission field (iODIAC)

The 30×30m improved emission field (iODIAC) and the other fields are shown in Figure 2. The emission gradients over the areas depicted by the impervious surface data were driven by population. Thanks to the use of 1×1km gridded population data, the blocky features are visible across the area (see Figure 2b). As expected, the emission mapping error is significantly reduced in iODIAC field compared to ODIAC, with iODIAC field being more closely related to Hestia, although emission gradients are modeled rather than being determined by sectoral information. We present a quantitative assessment of the iODIAC emissions in the following section by performing inversions over the city and by computing statistical metrics to evaluate the improved representation of urban CO_2 emissions.
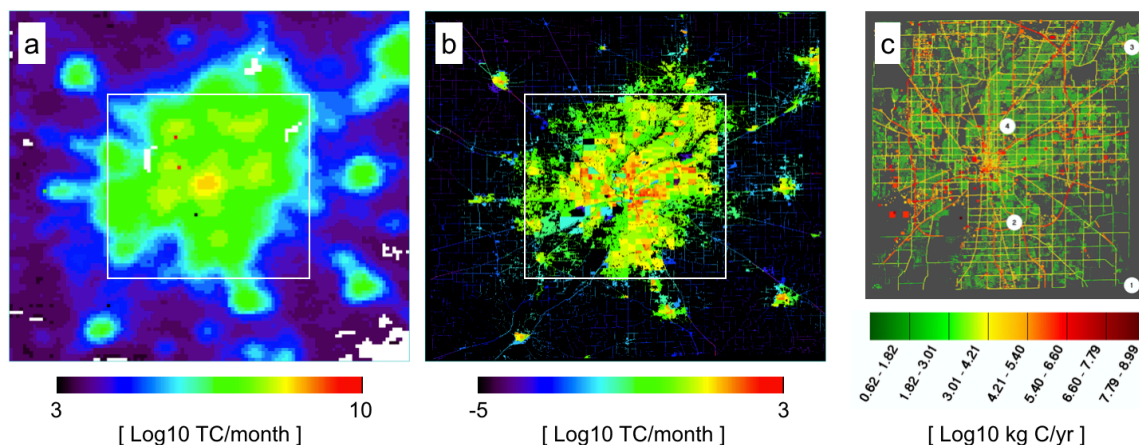
Figure 2. A comparison of three emission fields: 1×1km ODIAC (a), 30×30m improved ODIAC emission field (iODIAC) (b), and Hestia (c, Marion county only). The Hestia emission map was adopted from Gurney *et al*. (2012). The original high-resolution image is available at the Hestia project web page (http://hestia.project.asu.edu/index.shtml). The box on the ODIAC and iODIAC roughly indicates the Hestia domain.

3.3 Inversion results

Table 3 shows the summary of the 8-month inverse estimates over Indianapolis. Assuming Hestia is the best estimate of Indianapolis CO_2 emissions, the nightlight-based disaggregation emissions from ODIAC (only for non-point sources) are performing reasonably well for a middle-size city like Indianapolis. When the inversion was performed using the 30×30m improved emission field (iODIAC) as a priori, the inverse estimate differed by only 0.4 Mt/yr over 8 months (about 8% of the total emissions) compared to the Hestia-based inversion. The inversion result with ODIAC was slightly closer to the Hestia inversion result by 0.2 MtC/yr, within the uncertainty range of 0.6 MtC/yr. The spatial structure of the prior emissions has an indirect impact on the inverse emissions. Because the error variances are scaled with prior emissions, specific areas or points may be more or less susceptible to adjustments. Therefore, the differences in the total emissions will depend on the presence of sources near the observation locations which defines the degree of freedom of the prior emissions (i.e. error variances of the prior emissions). Overall, the sharp spatial emission gradients in iODIAC affected the whole-city inverse emissions producing a lower estimate over the entire period (lower by 0.17 MtC/yr). Assuming that iODIAC emissions represent the urban area more accurately than ODIAC, this result shows the sensitivity of the top-down estimate to the fine-scale structure as described by the prior emissions.

9

Table 2. A summary of three inversion results with different prior emission fields. Values are the total emissions from the study domain, given in the unit of MtC/yr. *Values are taken from Lauvaux *et al.* (2016).

Prior emission	Hestia* (MtC/yr)	ODIAC* (MtC/yr)	iODIAC – this study (MtC/yr)
A priori	4.56	4.12	4.15
A posteriori	5.5	5.3	5.13

Figure 3 shows the prior and posterior emission fields for the three inversion cases, i.e. inv_{Hestia}, inv_{ODIAC} and inv_{iODIAC} emissions. Although the total inv_{iODIAC} emission estimate differs from inv_{Hestia}, the two inverse emission distributions shared major spatial patterns especially with high emissions. The correlation with Hestia was increased from 46% to 52% and the Mean absolute Error (MAE) was reduced by 14% compared to inv_{ODIAC}. Both statistics are significant considering that the increased resolution of iODIAC artificially decreases the correlation (i.e. increases the MAE) due to misplacements of larger gradients in iODIAC. Smoother structures in ODIAC tend to have better correlations, attributable to smaller spatial gradients. We also note here that the power plant emissions were removed to avoid artificially high correlation values (the three maps share identical power plant information). Figure 3 illustrates the high resemblance between Hestia and iODIAC (upper row, left and right panels) compared to the smoothed pattern of emissions in ODIAC (upper row, middle panel). The inversion shows more diffuse emission corrections when using ODIAC (lower row, middle panel), while emission adjustments are guided by the spatial patterns in the IODIAC prior field and the error variances constructed accordingly (lower row, right panel).
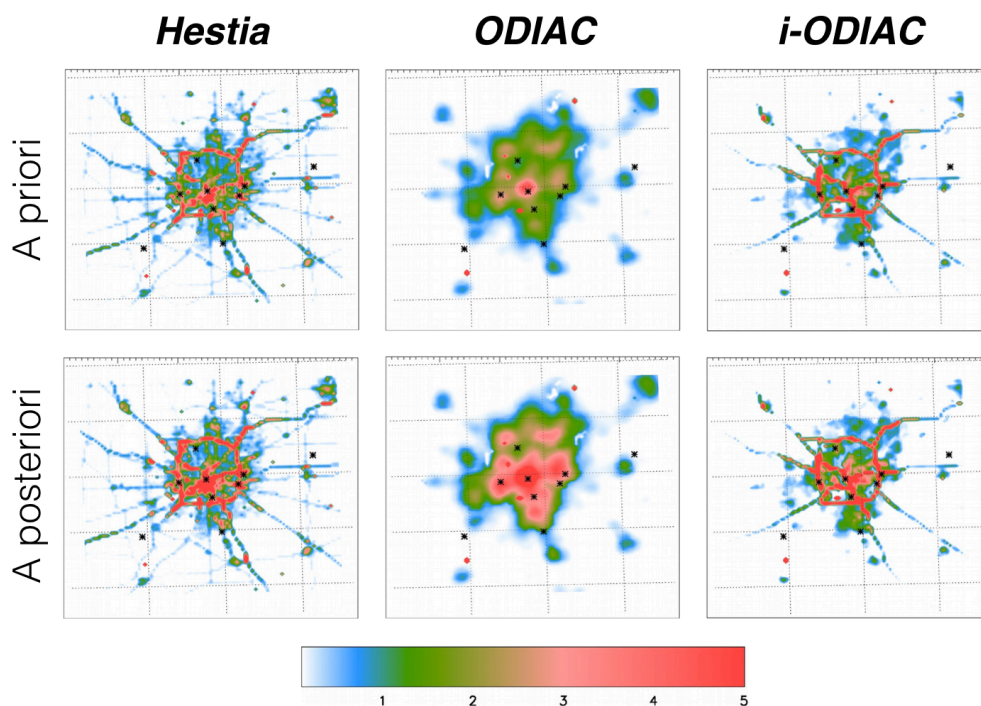
Figure 3. Spatial distributions of a priori (upper) and a posteriori (lower) emissions over Indianapolis, IN. Emission corrections were obtained at a 1×1 km resolution. Values are given in the unit of ktC/yr.

In Figure 4, the temporal variations in the posterior emissions are shown. As shown in previous inversion cases by Lauvaux *et al*. (2016), atmospheric data constrain the temporal variability while prior emissions have no significant impact on the inverse 5-day variations. The inverse results confirm that while spatial information remains a limiting factor despite the large number of towers over the city, temporal variations in the emissions being primarily constrained by observations rather than a priori information. Therefore, the lack of diurnal and sub-monthly variability in iODIAC is overcome by the observational constraint. This result is discussed further in Section 4.3 with potential implications for the development of future high resolution EI's.
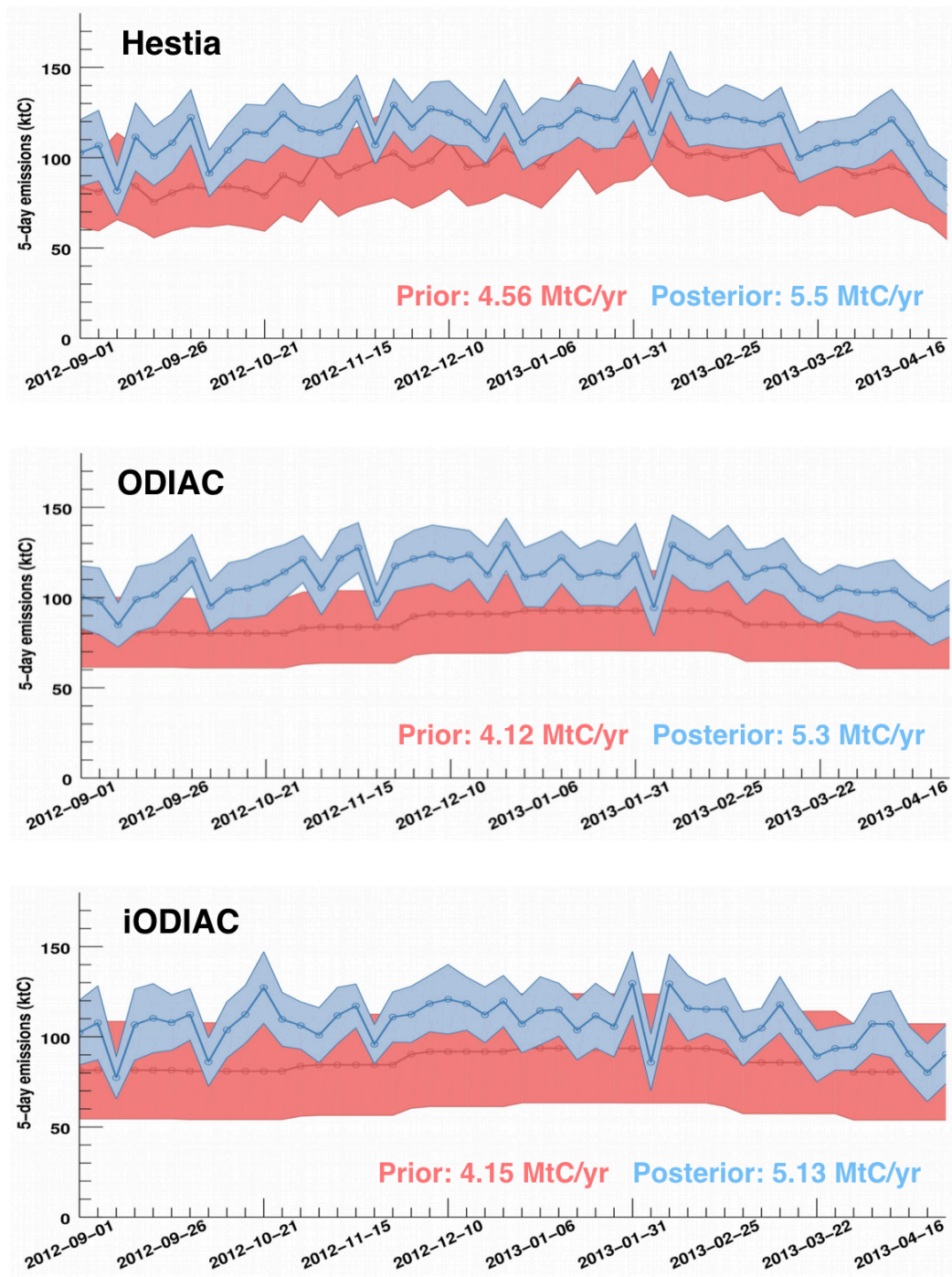
Figure 4. Time series of a priori (in pink) and a posteriori (in blue) emissions of CO_2 aggregated over the 9 counties surrounding Indianapolis using Hestia (top), ODIAC (middle), and iODIAC (bottom) as prior emissions.

We calculated the model-observation mismatch for the three inversion cases as a measure of the goodness-of-fit before and after inversion. Because the prior errors are fairly similar over the whole city, this result illustrates the capability of the inversion to fit the observed mole fractions and therefore the quality of the prior. If the prior structures are inconsistent with the gradients in the atmospheric observations, the goodness-of-fit will not improve after the inversion. Table 4 summarizes the values calculated from all the atmospheric measurements used in the inversion. We found that both iODIAC and inv$_{iODIAC}$ showed smaller model-observation mismatch compared to ODIAC and inv$_{ODIAC}$ emissions (-0.382 ppm vs. -0.487 ppm after inversion, and -0.819 ppm vs. -1.05 ppm before inversion), with iODIAC being further away than the Hestia case. This result confirms that iODIAC emission distribution is closer to that of Hestia, allowing the inversion to improve the fit to the atmospheric observations, which indirectly confirms a better distribution of the posterior emissions. The authors would like to highlight that, unlike the Hestia case, weekly to diurnal temporal patterns were not applied to neither ODIAC nor iODIAC.

Table 3. A prior and posterior model-observation mismatch. Values are calculated from all the measurements used in the inversion. Values are given in the units of ppm.

Prior emissions	Hestia (ppm)	ODIAC (ppm)	iODIAC – this study (ppm)
A priori	-0.769	-1.05	-0.819
A posteriori	-0.279	-0.487	-0.382

We further looked at model-observation mismatch for each tower assimilated in the inversion. Figure 5 shows the model-observation mismatch on a per-tower basis. In this analysis, only the posterior fit was used. The fit of Hestia emissions are available in Miles et al. (same issue). Here we only consider the fit to the posterior emissions. This analysis revealed that the posterior model-observation goodness-of-fit are similar or even better with inv$_{iODIAC}$ compared to inv$_{Hestia}$ emissions for most of the sites, except for sites #04 and #12 which are located on the south side of the city. For the site within the beltway (site #02, 03, 05, 07, and 10) where the emissions are most intense, the iODIAC case outperformed the other two cases. For site #04, the model-observation fit is similar for the three cases, indicating a missing adjustment in all cases. For site #12, the inv$_{ODIAC}$ and inv$_{iODIAC}$ model-observation differences are much larger than for the Hestia case.
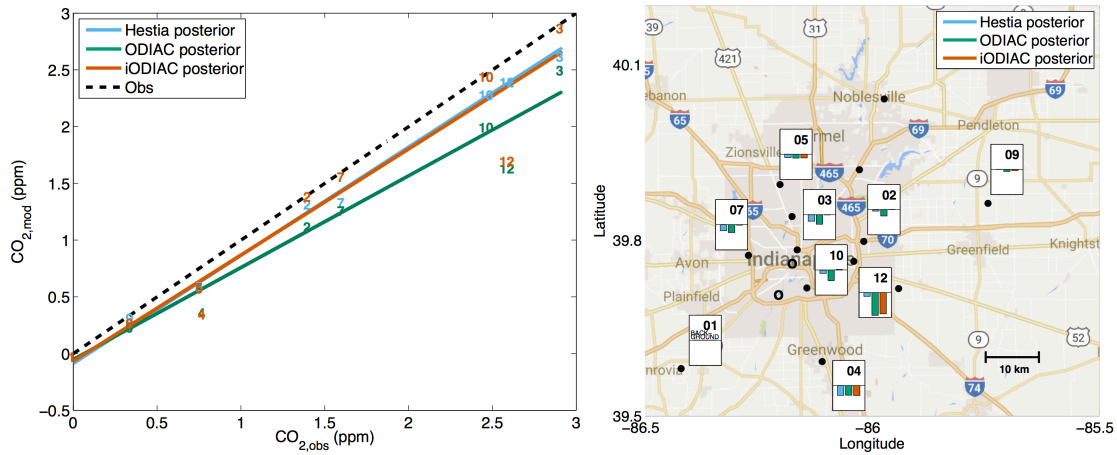
Figure 5. Posterior model-observation mismatch at nine INFLUX towers. Left: Modeled CO_2 enhancement as a function of observed CO_2 enhancement for the Hestia prior (blue), ODIAC posterior (green), iODIAC posterior (orange), and the 1-to-1 line (black dashed). Numbers indicate data point for individual sites. Right: Posterior model-observation mismatch at nice INFLUX towers for the Hestia posterior (blue), ODIAC posterior (green), iODIAC posterior (orange). The site number is shown in the upper right corner of each plot and the black circles indicate the locations of the sites. Open black circles indicate the location of the power plants within the city. The y-axis for each plot extends from -1 to +1 ppm CO_2. The observation are not available for this time period at Site 06, 08, 11 and 13.

4. Current limitations and future perspectives

Given the use of generic geospatial data that are available globally, our downscaling approach is applicable to any city in a systematic and timely manner, although the accuracy of the disaggregation method could vary due to errors/biases from larger scale EIs and/or solely due to the potential regional errors/biases in emission disaggregation. The use of very high-resolution satellite-driven data such as impervious surface data for emission mapping can be computationally expensive. For similar studies over multiple cities, the collection of impervious data for urban emissions only represents a small fraction of the surface of the globe which decreases significantly the amount of data and processing of such application. As pointed out by Lauvaux *et al*. (2016), error quantification and characterization for city scale inversion is often extremely difficult to implement due to the lack of information and the computational expense when considering large volume of data in EI's. Our approach could also provide a limited but meaningful opportunity to perform error quantification and characterization by providing alternative emission field to be compared. Thus, the authors believe that emission downscaling approach will help informing city emissions in a global framework for city top-down MRV, especially with future space-based carbon-observing missions. Here we discuss current limitations and future perspectives of this study in a context of city MRV implementation.

14

4.1 Emission information

As pointed out earlier, the lack of EI reported by cities is a fundamental, limiting factor in city MRV. Although the authors believe that development of a fine-grained EI such as Hestia is an ideal way to accurately quantify city emissions and inform top down methods in a city MRV framework, emission accounting for cities via compilation of EIs needs to be more commonly available and following existing guidelines, such as the Global Protocol for Community-Scale Greenhouse Gas Emission Inventories (GPC, http://www.ghgprotocol.org/city-accounting). With sector-specific information, more accurate emission modeling can be implemented instead of making crude assumptions about sectoral contributions (e.g., applying national-level sectoral distributions or averaged city sectoral fractions to every city). Spatially defined EIs or geolocation information will also greatly support the introduction of the complexity and the diversity of anthropogenic sources in the resulting emission field at fine scale.

The quality of EI is often correlated with the goodness of statistical data collected from various institutions or directly from private organizations (e.g., Olivier and Peters 2002; Marland, 2008; Andres *et al*., 2012). Most of the countries that are thought to be producing lower quality EIs are unlikely to be able to compile high-accuracy EIs at the city scale. Collecting accurate data at large scales for aggregated EIs (e.g., national and province levels) remains more practical than city-scale emissions. Therefore, the construction of fine-grained top down estimates to support city-scale EIs is an attractive solution to produce more accurate estimates in any country, and possibly offer a monitoring of the reported emissions, consistent with estimates from larger scales. As an example, Guan *et al.* (2012) reported a 1Gt CO_2 difference between estimates based on national and province level statistics in China.

4.2 Disaggregation (Mapping) error

Initially, the agreement between ODIAC and Hestia total emissions suggests that the downscaling approach can give us a reasonable estimate for whole-city emissions (within 10%). However, disaggregation (mapping) error can be more significant when moving to higher spatial resolutions. Especially at very high spatial resolution, source locations have to be determined rather than estimated or approximated using proxy data. As seen in the emission pattern, ODIAC provides maps of CO_2 emissions over areas that are unlikely to be emitting (see Figure 2). Other than the resolution mismatch (1km vs. 30m), the underlying nightlight data used in ODIAC, provided by the Defense Meteorological Satellite Program (DMSP) Operational Linescan System (OLS) nightlight data (https://ngdc.noaa.gov/eog/dmsp.html), have known limitations (e.g., Elvidge *et al.*, 2013). The authors are working on applying new nightlight environmental product

developed from data collected by Visible Infrared Imaging Radiometer Suites (VIIRS) on Suomi National Polar-orbiting Partnership (NPP) satellite (Román and Stokes, 2015) to the ODIAC emission model (Oda *et al.*, 2016). There are a number of improvements in VIIRS over the previous instrument which will mitigate the mapping error originating from the use of current nightlight data.

Although the satellite-driven data used in this study for downscaling (e.g., nightlights and impervious surface data) turned out to be useful for determining source regions within a city, nightlights intensity, or development density in impervious surface data, does not fully explain any emission spatial gradients within the emitting area. In this study, we used population data to model the spatial emission gradient. In future study, we will examine the impact of emission gradients on the posterior emission estimates constrained by other proxies, which could be a source of bias in the current inversion setup.

Given the absence of other EI estimates, the evaluation of biases in the emission field remains unachievable. However, geolocation information used to map the emissions can be addressed from various data sources. Although emissions estimates could be significantly biased for sources such as power plants and transportation, we could determine the precision of the geolocation at a minimum (e.g., locations of power stacks and road networks). This first step is critical for city-scale inversions because atmospheric data are unlikely to determine the locations of large sources within the city limits. The verification of intense sources is also limited to few proxies such as public information from Google Map/Earth. However, the limited numbers of large point sources remain manageable within each city compared to the national scale EIs (e.g., Oda and Maksyutov, 2011). This type of error/uncertainty has been discussed in other studies (e.g., Oda and Maksyutov, 2011; Woodard *et al.*, 2015)

4.3 Time profiles

In this study, we focused on the impact of spatial emissions distributions on the inverse emissions without including any temporal variations in the a priori beyond monthly time scale (except Hestia). The seasonality in ODIAC is taken from estimates made by the Carbon Dioxide Information Analysis Center (CDIAC) at Oak Ridge National Laboratory (Oda *et al.*, 2016). The CDIAC seasonality is based on national monthly fuel statistics, rather than subnational (e.g., state) monthly statistics. Thus, the actual subnational seasonality might be different. According to GPC inventory guidelines, future products may include an annual (i.e. 12 month) inventory. The development of monthly emissions would greatly improve the current level of information in EIs. Climatology may also be used for modeling purposes such as Nassar *et al.* (2010). The response to environmental conditions and human events (e.g., regular weekday/weekends vs. holidays) should be detectable and therefore quantifiable, if applied. Overall, the authors would like to

16

highlight that the inversion with iODIAC was able to show a very good match with the atmospheric observations comparable to Hestia inversion case over an 8-month period. Future work will aim to assess the impact of temporal profiles in the emissions relative to the impact of finer spatial distributions.

4.4 Error specification

The lack of the error quantification/characterization in the fine-grained emission dataset was discussed by Lauvaux *et al.* (2016). As mentioned earlier, many sources of uncertainties can affect the emissions and need to be carefully considered depending on the flux resolution (e.g., time and space) of interest. Most of the emission datasets are based on disaggregation of emissions (e.g., CDIAC, EDGAR) where proxy data are used at many different levels. The proxy data are used to approximate the spatial emissions and thus are usually not appropriate at urban scales where individual processes are identifiable. Emission intercomparison may not be highly meaningful but given the lack of physical measurements or EIs constructed at comparable spatial resolutions, model intercomparison remains valid. In the current inversions, the absence of definition for emissions errors is critical, impairing the ability of top down methods (Lauvaux *et al.*, 2016). Given the relatively good performance of iODIAC and the presence of detailed spatial structures, the assessment of emissions errors is a critical objective for urban inversions to improve both the distribution and the total emissions of the city.

5. Conclusions

We present the first space-based emission field at fine resolution to inform a top-down urban-scale framework. Following the INFLUX inversion case with a global 1×1 km ODIAC fossil fuel CO_2 emission dataset as a prior, we further improved the 1×1 km emission field from the global ODIAC dataset to describe higher levels of emission granularity at the city-scale such as roads and point sources, often missing in coarser resolution products. We approached city emission fields with three types of geometrical objects to represent the principal emission sector components: point, line and diffused (area) emission sources. While preserving the point source information in the ODIAC dataset, we disaggregated the non-point source emissions using geospatial dataset such as global road network data and satellite-data driven surface imperviousness data to generate a 30×30 m resolution emission field, comparable to the spatial scale of Hestia. Our disaggregation theoretically can be applied to any global cities and provide an emission estimate with spatial distributions even EI are not compiled locally. The posterior emission estimate summed over the whole city was about 5.1 MtC/yr and remains statistically similar to the previous inversion using ODIAC (5.3MtC/yr, as reported by Lauvaux *et al.*, 2016). However, the inversion with the 30×30 m emission field yielded flux corrections with major

spatial patterns matched with those of the inverse using a state-of-the-art building-level emission product, and the optimized model-observation mismatches were similar across the city despite the absence of hourly variability in the prior emissions.

Although emission disaggregation is not often the best approach to inform emissions at a high spatial resolution, our result showed that the use of the geospatial data allowed us to improve the prior emission spatial structure within the city and the potential for providing city emissions where fine-grained emissions data are not available. Beyond the simple mapping of GHG emissions, we quantify here the indirect gain of information by using better-informed a priori emissions, further increasing the potential of the top down approach. This combined approach is particularly useful as fine-grained emission products like Hestia are rarely available for a vast majority of the large metropolitan areas across the globe. Currently, city scale emissions are reported for some cities within local climate action such as Compact of Mayors (https://www.compactofmayors.org/). If we were to start with such activities using atmospheric information, the reported EI (often without spatial distributions) needs to be disaggregated, in order to be incorporated into models. Our method offers a potential approach to a global verification system of city emissions (MRV) using a disaggregation method and an atmospheric inversion system at the urban scale. Given the availability of generic geospatial data, our approach could provide fine-scale city emissions in various locations as future CO_2 observations from ground-based or space missions become more systematically available.

References

Andres RJ, Gregg JS, Losey L, Marland G, Boden TA. 2011. Monthly, global emissions of carbon dioxide from fossil fuel consumption, Tellus 63B: 309-327.

Andres RJ, Boden TA, Bréon F-M, Ciais P, Davis S, et al. 2012. A synthesis of carbon dioxide emissions from fossil-fuel combustion, Biogeosciences 9, 1845-1871. doi:10.5194/bg-9-1845-2012.

Andres RJ, Boden TA, Higdon DM. 2016. Gridded uncertainty in fossil fuel carbon dioxide emission maps, a CDIAC example, Atmos. Chem. Phys. 16, 14979-14995. doi:10.5194/acp-16-14979-2016.

Asefi-Najafabady S, Rayner PJ, Gurney KR, McRobert A, Song Y. et al. 2014. A multiyear, global gridded fossil fuel CO_2 emission data product: Evaluation and analysis of results. J. Geophys. Res. Atmos. 119, 10213–10231. doi:10.1002/2013JD021296.

Bovensmann H, Buchwitz M, Burrows, JP, Reuter, M, Krings, T. et al. 2010. A remote sensing technique for global monitoring of power plant CO_2 emissions from space and related applications. Atmos. Meas. Tech. 3: 781-811.

Buchwitz M, Reuter M, Bovensmann H, Pillai D, Heymann J. et al. 2013. Carbon Monitoring Satellite (CarbonSat): assessment of atmospheric CO2 and CH4 retrieval errors by error parameterization. Atmos. Meas. Tech. 6: 3477-3500, doi:10.5194/amt-6-3477-2013.

Center for International Earth Science Information Network - CIESIN - Columbia University, and Information Technology Outreach Services - ITOS - University of Georgia. 2013. Global Roads Open Access Data Set, Version 1 (gROADSv1). Palisades, NY: NASA Socioeconomic Data and Applications Center (SEDAC). http://dx.doi.org/10.7927/H4VD6WCT.

Deng A, Stauffer D, Gaudet B, Dudhia J, Bruyere C. et al. 2009. Update on WRF-ARW end-to-end multi-scale FDDA system. *10th WRF User's workshop*, NCAR. Boulder, C.O. 14pp.

Duren RM and Miller CE. 2012. Measuring the Carbon Emissions of Megacities. Nature Climate Change 2: 560–562, doi:10.1038/nclimate1629.

Eldering A. 2015. The OCO-3 Mission: Overview of Science Objectives and Status, 2015 American Geophysical Union (AGU) Fall Meeting, San Francisco.

Elvidge CD, Baugh K, Zhizhin M, Hsu FC. 2013. Why VIIRS data are superior to DMSP for maping nighttime lights, Proc. the Asia-Pacific Advanced Network 35: 62-69, http://dx.doi.org/10.7125/APAN.35.7

Enting IG, Trudinger CM and Francey RJ. 1995. A synthesis inversion of the concentration and d13C atmospheric CO2, Tellus B 47: 35–52.

Feng S, Lauvaux T, Newman S, Rao, P., Ahmadov, R. et al. 2016. Los Angeles megacity: a high-resolution land–atmosphere modelling system for urban CO2 emissions, Atmos. Chem. Phys., 16, 9019-9045, doi:10.5194/acp-16-9019-2016.

Gately CK, Hutyra LR, Sue Wing I. 2015. Cities, traffic, and CO_2: A multi-decadal assessment of trends, drivers, and scaling relationships. Proc. Natl. Acad. Sci. USA. 112 (16) 4999-5004. doi: 10.1073/pnas.1421723112.

Guan D, Liu Z, Geng Y, Lindner S, Hubacek K. 2012. The gigatonne gap in China's carbon dioxide inventories. Nature Climate Change 2: 672–675.

Gurney KR, Mendoza D, Zhou Y, Fischer M, de la Rue du Can S, Geethakumar S. et al. 2009. The Vulcan Project: High resolution fossil fuel combustion CO_2 emissions fluxes for the United States. *Environment Science and Technology* 43: 5535–5541.

Gurney K, Razlivanov I, Song Y, Zhou Y. et al. 2012. Quantification of fossil fuel CO_2 emission on the building/street scale for a large US city. Environ. Sci. & Technol. 46: 12194-12202.

Gurney KR, Liang J, Patarasuk R, O'Keeffe D, Huang J. et al. 2016. Reconciling the differences between a bottom-up and inverse-estimated FFCO2 emissions estimate in a large US urban area, submitted to *Elementa*

Hutyra L, Duren R, Gurney KR, Grimm N, Kort E. et al. 2014. "Urbanization and the carbon cycle: Current capabilities and research outlook from the natural sciences perspective", *Earth's Future*, doi:10.1002/2014EF000255.

Janardanan R, Maksyutov S, Oda T, Saito M, Kaiser JW, Ganshin A, Stohl A, Matsunaga T, Yoshida Y, Yokota T. 2016. Comparing GOSAT observations of localized CO_2 enhancements by large emitters with inventory-based estimates, Geophys. Res. Lett. 43, doi:10.1002/2016GL067843.

Janssens-Maenhout G, Dentener F, Van Aardenne J, Monni S, Pagliari V, et al. 2012. EDGAR-HTAP: a Harmonized Gridded Air Pollution Emission Dataset Based on National Inventories. Ispra (Italy): European Commission Publications Office; 2012. JRC68434, EUR report No EUR 25 299 - 2012, ISBN 978-92-79-23122-0, ISSN 1831-9424

Kort EA, Frankenberg C, Miller CE, Oda T. 2012. Space-based observations of megacity carbon dioxide. Geophys. Res. Lett. 39: 17-22.

Kuenen J, Visschedijk A, Jozwicka M, Gon H. 2014. TNO-MACC_II emission inventory; a multi-year (2003– 2009) consistent high-resolution European emission inventory for air quality modelling, Atmos Chem Phys, 14(20), 10963–10976, doi:10.5194/acp-14-10963-2014.

Kurokawa J, Ohara T, Morikawa T, Hanayama S, Janssens-Maenhout G. et al. 2013. Emissions of air pollutants and greenhouse gases over Asian regions during 2000–2008: Regional Emission inventory in ASia (REAS) version 2, Atmos. Chem. Phys. 13: 11019-11058, doi:10.5194/acp-13-11019-2013.

Lauvaux T. et al. 2016. High-resolution atmospheric inversion of urban CO_2 emissions during the dormant season of the Indianapolis Flux Experiment (INFLUX), J. Geophys. Res. Atmos., 121, doi:10.1002/2015JD024473.

Liu Z. et al. 2015. Reduced carbon emission estimates from fossil fuel combustion and cement production in China, Nature 524: 335–8

Marland G. 2008. Uncertainties in Accounting for CO_2 From Fossil Fuels. J. Industrial Ecology, 12: 136–139. doi: 10.1111/j.1530-9290.2008.00014.x.

Miles NL. et al. 2016. Detectability and quantification of atmospheric boundary layer greenhouse gas dry mole fraction enhancements in an urban landscape: Results from the Indianapolis Flux Experiment (INFLUX) submitted to Elementa

Mills G. 2007. Cities as agents of global change. International Journal of Climatol. 27: 1849-1857.

Nassar R, Jones DBA, Suntharalingam P, Chen JM, Andres RJ. et al. 2010. Modeling global atmospheric CO_2 with improved emission inventories and CO_2 production from the oxidation of other carbon species. Geosci. Model Dev. 3: 689-716.

Nisbet E. and Weiss R. 2010. Top-down versus bottom-up, Science 328: 1241–1243. doi: 10.1126/science.1189936.

Oda T and Maksyutov S. 2011. A very high-resolution (1km×1km) global fossil fuel CO_2 emission emission inventory derived using a point source database and satellite observations of nighttime lights. Atmos. Chem. and Phys. 11: 543-556.

Oda T, Maksyutov S, Andres RJ. 2016. The Open-source Data Inventory for Anthropogenic CO_2 (ODIAC) fossil fuel emission model version 3.0 (ODIAC v3.0), submitted to Geosci. Model Dev.

Olivier JGJ. 2002. On the Quality of Global Emission Inventories: Approaches, Methodologies, Input Data and Uncertainties, PhD thesis University Utrecht, ISBN 90-393-3103-0

Olivier JGJ, Aardenne JAV, Dentener FJ, Pagliari V, Ganzeveld LN, Peters JAHW. 2005. Recent trends in global greenhouse gas emissions: Regional trends 1970–2000 and spatial distribution of key sources in 2000, J. Integr. Env. Sci. 2: 81–99. doi:10.1080/15693430500400345.

Olivier JGJ. and Peters JAHW. 2002. Uncertainties in global, regional, and national emissions inventories. In Non-CO2 greenhouse gases: Scientific understanding, control options and policy aspects, edited by: Van Ham J, Baede APM, Guicherit R, and WIlliams-Jacobse JFGM, Springer, New York, USA, 525–540.

Pacala SW. et al. 2010. Verifying Greenhouse Gas Emissions: Methods to Support International Climate Agreements. *Committee on Methods for Estimating Greenhouse Gas Emissions; National Research Council*, National Academy of Sciences, 124pp.

Patarasuk P, Gurney KR, O'Keeffe D, Song Y. Huang J. et al. 2016. Application of high-resolution fossil fuel CO2 emissions quantification to urban climate policy in Salt Lake County, Utah USA, Urban Ecosystems. DOI 10.1007/s11252-016-0553-1.

Polonsky IN, O'Brien DM, Kumer JB, O'Dell CW. and the geoCARB Team:. 2014. Performance of a geostationary mission, geoCARB, to measure CO2, CH4 and CO column-averaged concentrations, Atmos. Meas. Tech. 7: 959-981, doi:10.5194/amt-7-959-2014.

Rayner PJ, Raupach MR, Paget M, Peylin, P, Koffi E. 2010. A new global gridded data set of CO2 emissions from fossil fuel combustion: Methodology and evaluation. J. Geophys. Res. 115, D19306, doi:10.1029/2009JD013439.

Richardson SJ, Miles NL, Davis KJ, Lauvaux L, Martins DK. et al. 2016. CO2, CH4, and CO tower in situ measurement network in support of the Indianapolis FLUX (INFLUX) Experiment. submitted to *Elementa*

Román MO and Stokes EC. 2015. Holidays in Lights: Tracking cultural patterns in demand for energy services. Earth's Future. doi:10.1002/2014EF000285.

Streets D. et al. 2003. An inventory of gaseous and primary aerosol emissions in Asia in the year 2000, J. Geophys. Res., 108(D21), 8809, doi:10.1029/2002JD003093.

Turnbull JC. et al. 2015. Toward quantification and source sector identification of fossil fuel CO_2 emissions from an urban area: Results from the influx experiment. J. Geophys. Res. Atmos. *120*: 292–312, doi:10.1002/2014JD022555.

Uliasz M. 1994. Lagrangian particle modeling in mesoscale applications, in Environmental Modelling II, edited by P. Zanetti, Computational Mechanics Publications, pp.71–102.

Woodard D, Branham M, Buckingham G, Hogue S, Hutchins M. et al. 2014. A spatial uncertainty metric for anthropogenic CO_2 emissions", Greenhouse Gas Measurement and Management (2014) 2-4, 139-160.

Contributions

TO and TL conceived and designed the study, implemented the analysis and drafted the manuscript. NLM and SJR acquired atmospheric CO_2 data. KRG developed and provided Hestia emission dataset. PR and DL contributed to geospatial data processing. All the authors contributed to improve the manuscript.

Acknowledgment

Funding Information

Competing information

The authors have declared that no competing interest exists.

Data accessibility statement

The ODIAC global emission dataset is available at
http://db.cger.nies.go.jp/dataset/ODIAC/. "Hestia" fine-grained emission dataset is avaialbe from
http://hestia.project.asu.edu/. The Global Roads Open Access Data Set (gROADS) v1 is available
from http://sedac.ciesin.columbia.edu/data/set/groads-global-roads-open-access-v1. National
Land Cover Dataset (NLCD) 2011 is available from http://www.mrlc.gov/nlcd2011.php. The
atmospheric CO_2 tower data used in this study are available at http://sites.psu.edu/influx/data/.